Supporting Information

Multiplexed Detection of Respiratory Pathogens Using Portable Device Combining a CREM Strategy

Xijuan Gu[b,c], Anli Pan[b], Lingwei Wu[b], Jing Zhang[b], Zixun Xu[b], Tao Wen[b], Miaomiao Wang[b], Xiuying Shi[d], Li Wu*[a], Yuling Qin*[b]

[a] School of Life Science, Nantong University, Nantong, Jiangsu 226019, P. R. China.

[b] Nantong Key Laboratory of Public Health and Medical Analysis, School of Public Health, Nantong University, Nantong, Jiangsu 226019, P. R. China.

[c] Xinglin College, Nantong University, Qidong, Jiangsu 226236, P. R. China.

[d] Department of Laboratory Medicine, Affiliated hospital of Nantong University, No. 20, Xisi Road, Nantong 226001, Jiangsu, China.

*Corresponding authors:

Tel: +86-513-55003046;

E-mail: Li Wu (wuli8686@ntu.edu.cn); Yuling Qin (ylqin@ntu.edu.cn)

Contents:

1. Materials and Methods

1.1 Reagents and materials

The basic ERA kit was purchased from Suzhou GenDx Biotech (Suzhou, China). LbCas12a nuclease was offered by Tolo Biotech Co., Ltd (Shanghai, China). QuickExtractTM DNA extraction solution was provided as a complimentary sample by Zhong Bei Lin Ge Biotech Co., Ltd (Qingdao, China). The ChamQ SYBR qPCR Master Mix was acquired from Vazyme Biotech Co., Ltd (Nanjing, China). Acrylamide, Tris Base, NaCl, and N, N'-Methylenebisacrylamide were supplied by Aladdin Biochemical Technology Co., Ltd (Shanghai, China). Ammonium persulfate and N, N, N', N'-Tetramethylethylenediamine (TEMED) were offered by Macklin Biochemical Co., Ltd (Shanghai, China). Silver nitrate ($AgNO_3$) and sodium hydroxide (NaOH) were provided by Lingfeng Chemical Reagents Co., Ltd (Shanghai, China). RNase-free water was purchased from Beyotime Biotechnology (Shanghai, China). The 3D printer was acquired from Creative 3D Technology Co., Ltd (Shenzhen, China). The UV LED panels (5V, 2W), excitation filters (550/60 nm, 605/55 nm, and 660/40 nm) and heaters were ordered from Alibaba. *S. pneumoniae, H. influenzae, M. pneumoniae, S. agalactiae, S. aureus, E. coli, K. pneumoniae, and P. aeruginosa* were obtained from the Affiliated Hospital of Nantong University.

Native polyacrylamide gel electrophoresis (PAGE) was performed on an electrophoresis apparatus (DYY-6D, China) and visualized on a gel imaging facility (Tanon, China). Fluorescence (FL) detections were measured with an FS5 fluorescence spectrofluorometer (Edinburgh Instruments Ltd., UK). Real-time fluorescence PCR assay was performed using the fluorescence quantitative PCR instrument (Bio-Rad, USA).

1.2 DNA extraction and isothermal amplification

Genomic DNA was extracted using QuickExtractTM DNA extraction solution, according to manufacturer's instruction. DNA extraction requires heat treatment to lyse pathogens, release the DNA, and degrade compounds that inhibit amplification. Following heat treatment, the DNA extracted from pathogen was stored at -20 °C for subsequent experiments.

Enzymatic recombinase amplification (ERA) technique is an upgraded version of the recombinase polymerase amplification (RPA). It achieves rapid nucleic acid amplification through the simultaneous action of multiple functional proteins under constant temperature conditions, without thermal cycling [1]. The ERA reaction was performed in accordance with the instruction manual of a basic ERA nucleic acid amplification kit. The product was used as a template for the Cas12a/engineered crRNA detection.

1.3 Primer, probes, and engineered crRNA preparation

The primers were designed according to the *cpsB* gene of *S. pneumoniae* (GenBank accession JN642323.1), the *siaT* gene of *H. influenzae* (GenBank accession NC_007146.2), and the *P1* gene of *M. pneumoniae* (GenBank accession AF290001.1) using Primer Premier5.0 software. All primers and probes were synthesized by Sangon Biotech Co., Ltd (Shanghai, China) and shown in Table S1. The engineered crRNA of distinct pathogens was directly synthesized and purified using RNase-free HPLC by Sangon Biotech.

1.4 Gel electrophoresis

A polyacrylamide gel was prepared using a solution consisting of 30% acrylamide, 0.1% ammonium persulfate, 0.01% tetramethyl ethylene diamine, and TBE buffer (89.2 mM Tris, 89.2 mM boric acid, and 0.2 mM EDTA). Subsequently, 6 μL of nucleotide samples with 1 μL loading buffer were loaded onto the gel. Electrophoresis was carried out in TBE buffer at room temperature for one hour at 120 V. The gel was fixed sequentially in 10% ethanol and 1% nitric acid for 5 minutes each, followed by agitation in 0.2% $AgNO_3$ for another 5 minutes. After two rinses with ultrapure water, the gel was stained with a solution containing 0.4% formaldehyde and 1.2% NaOH until distinct strips were visible.

1.5 Real-time PCR of respiratory pathogens

A commercial real-time PCR kit was utilized to detect *S. pneumoniae*, *H. influenzae*, and *M. pneumoniae*. The 20 μL reaction system consisted of 10 μL of 2×SYBR qPCR Master Mix, 200 nM forward and reverse primers, and varying concentrations of genomic DNA. The Bio-Rad CFX96 Mestro instrument was

employed for the reaction. The real-time quantitative PCR amplification process involved an initial pre-heating step at 94 ℃ for 3 minutes, followed by 40 cycles with each cycle consisting of 94 ℃ for 10 seconds and 60 ℃ for 30 seconds. Subsequently, a melting curve analysis was conducted. The kit's criteria for interpretation were as follows: a Ct value of ≤35 was considered positive, while a Ct value of >35 was deemed negative. The results of the real-time quantitative PCR detection for the three pathogens are presented in Figures S17, S18, and S19.

1.6 Statistical analyses

Every result was displayed as mean ± SD. A two-tailed Student’s t-test was used to establish statistical significance. The *p*-values below 0.05 were regarded as significant.

2 Supplementary Figures

2.1 PAGE analysis of the original crRNA and the engineered crRNA.

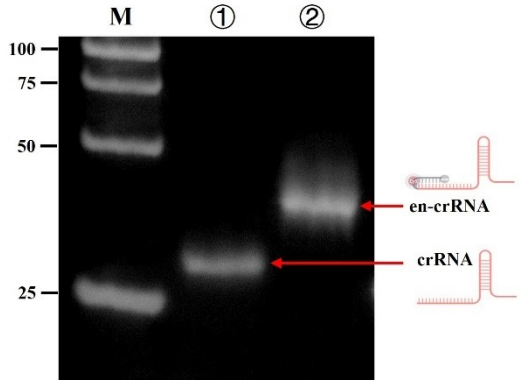

Figure S1. PAGE analysis of the original crRNA and the engineered crRNA. Lane M represents the DNA marker. Lane 1 represents the original crRNA, while Lane 2 represents the en-crRNA.

2.2 Schematic illustration in a single reaction.

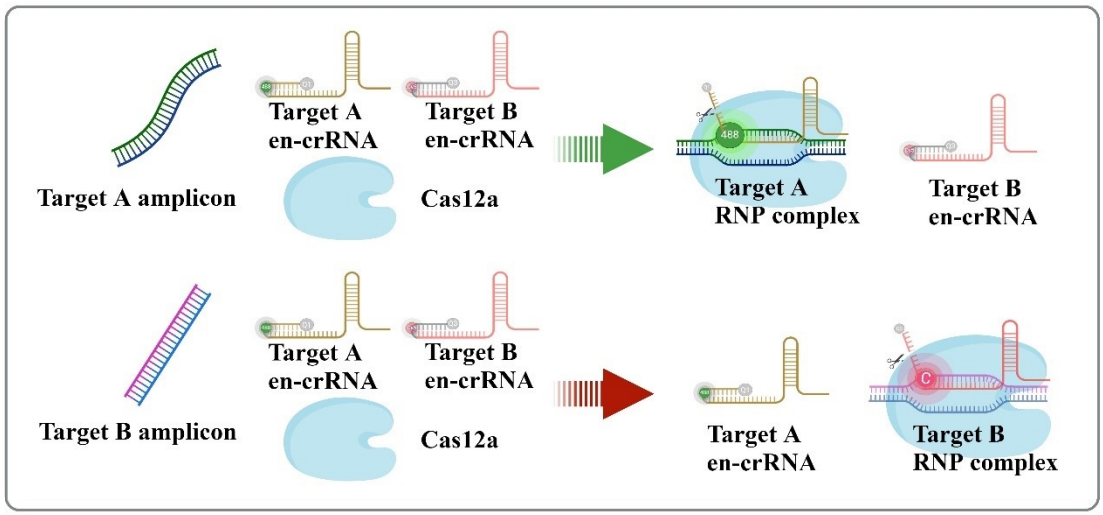

Figure S2. Schematic illustration of the engineered crRNA-assisted multiplex detection in a single reaction. Illustrations created by Biorender.

2.3 Establishment of the single-tube multiplex detection.

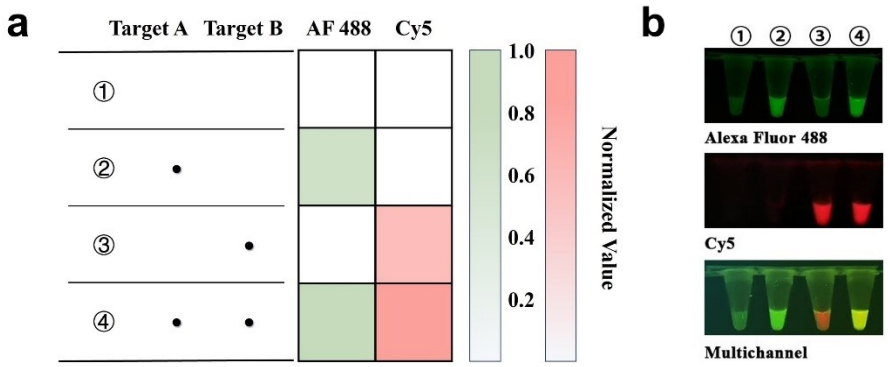

Figure S3. Establishment of the single-tube multiplex detection. (a) Fluorescence signals of the CREM system in the absence and presence of target A and/or target B. (b) Fluorescence images of reaction tubes after the detection of synthetic targets using the CREM system.

2.4 . Sensitivity of the CREM system.

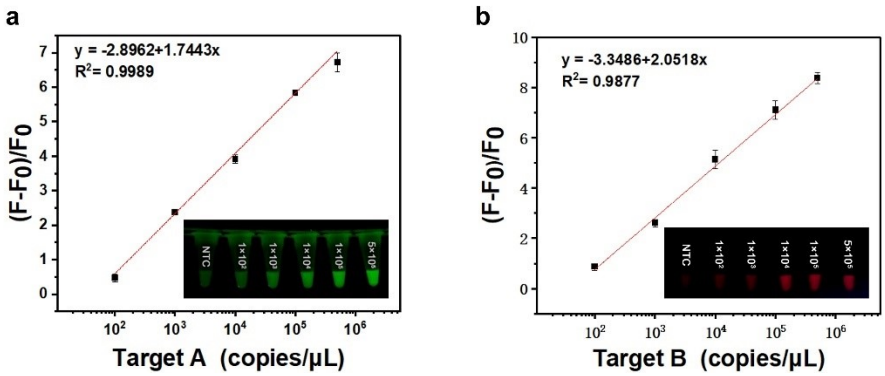

Figure S4. Sensitivity of the CREM system for the detection of (a) target A and (b) target B. *F* represents the fluorescence intensity obtained from the sample, while F_0 represents that obtained from NTC. Values represent mean ± standard deviation (n=3).

2.5 Optimization of the CREM assay.

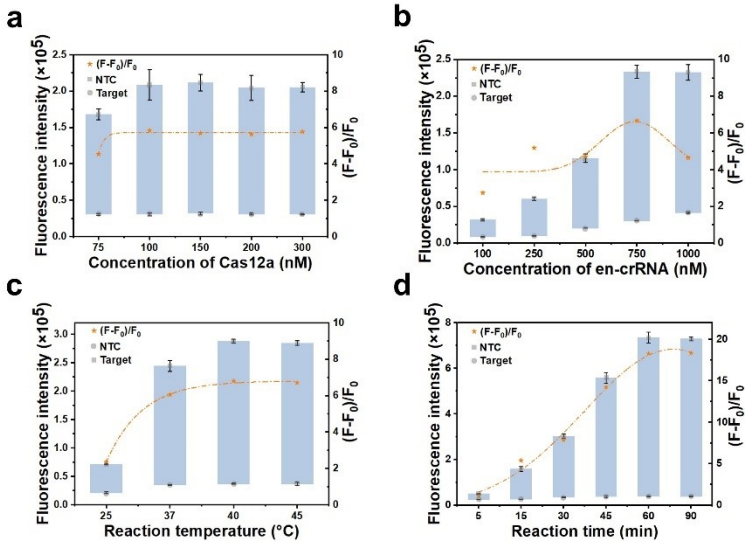

Figure S5. Optimization of the CREM assay. Fluorescence response towards target dsDNA using different concentrations of Cas12a (a) and the engineered crRNA (b). (c) Optimization of the different reaction temperature. (d) Optimization of the Cas12a cleavage time. The target dsDNA concentration was 1×10^5 copies/μL. Values represent mean ± standard deviation (n=3).

2.6 Reaction buffer optimization for the CREM system.

a

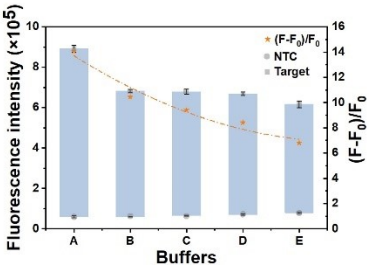

b

No.	Names	Components
A	TOLO Buffer	Tolo Biotechnology
B	ThermoPol Buffer	20 mM Tris-HCl; 10 mM $(NH4)_2SO_4$; 10 mM KCl; 2 mM $MgSO_4$; 0.1% Triton X-100; pH 8.8@25°C
C	NEBuffer 3.1	100 mM NaCl; 50 mM Tris-HCl; 10 mM $MgCl_2$; 100 μg/ml BSA; pH 7.9@25°C
D	NEBuffer 2.1	50 mM NaCl; 10 mM Tris-HCl; 10 mM $MgCl_2$; 100 μg/ml BSA; pH 7.9@25°C
E	NEBuffer 1.1	10 mM Bis-Tris-Propane-HCl; 10 mM $MgCl_2$; 100 μg/ml BSA; pH 7@25°C

Figure S6. Reaction buffer optimization for the CREM system. (a) The detection efficiency of the CREM detection system is compared using five distinct buffers. Values represent mean ± standard deviation (n=3). (b) Five buffers using in the CREM assay.

2.7 . Optimization of the engineered crRNA composition.

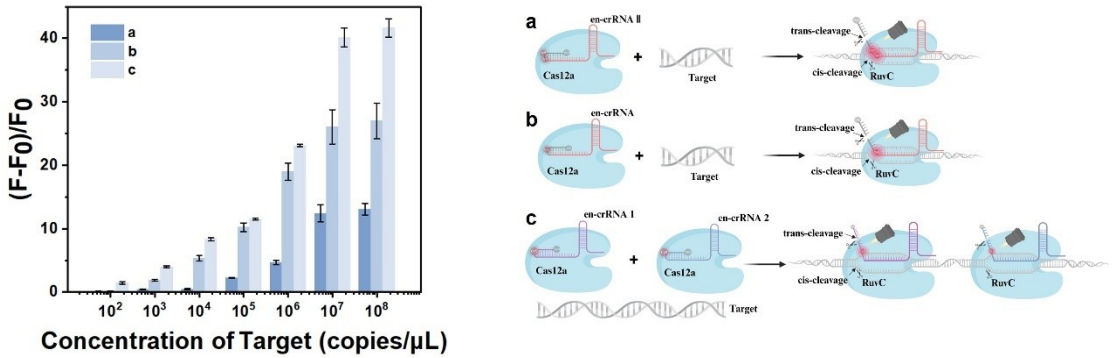

Figure S7. Optimization of the engineered crRNA composition. Plots depicting the reaction of Cas12a with Cy5 double-labeled en-crRNA (a), individual labeled en-crRNA (b), and combining multiple en-crRNAs (c). Values represent mean ± standard deviation (n=3). Illustrations created by Biorender.

2.8 Combination of multiple en-crRNAs.

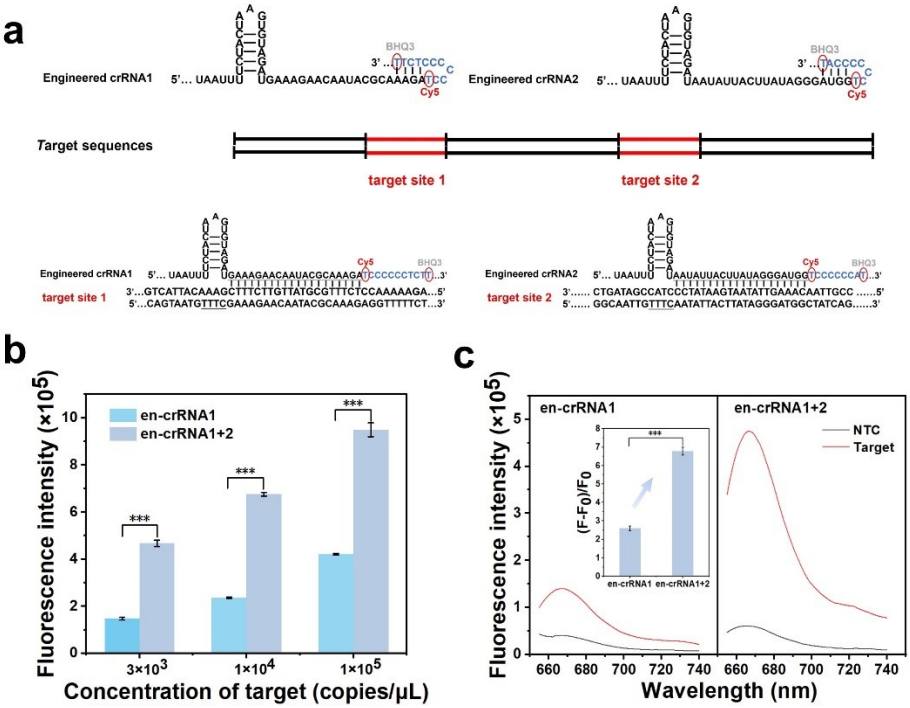

Figure S8. Combination of multiple en-crRNAs to improve the sensitivity of the CREM system. The en-crRNA1 and en-crRNA2 were designed (a) to detect the target individually and in combination at three distinct concentrations (b). (c) Comparison of the fluorescence intensity and the $(F - F_0)/F_0$ ratio between the individual labeled en-crRNA and the combining en-crRNAs assay. Values represent mean ± standard deviation (n=3). The statistical significance of the data in b and c (inset) was determined using two-tailed unpaired Student's t-test (*** $p < 0.001$).

2.9 Schematic illustrations of three gene en-crRNAs.

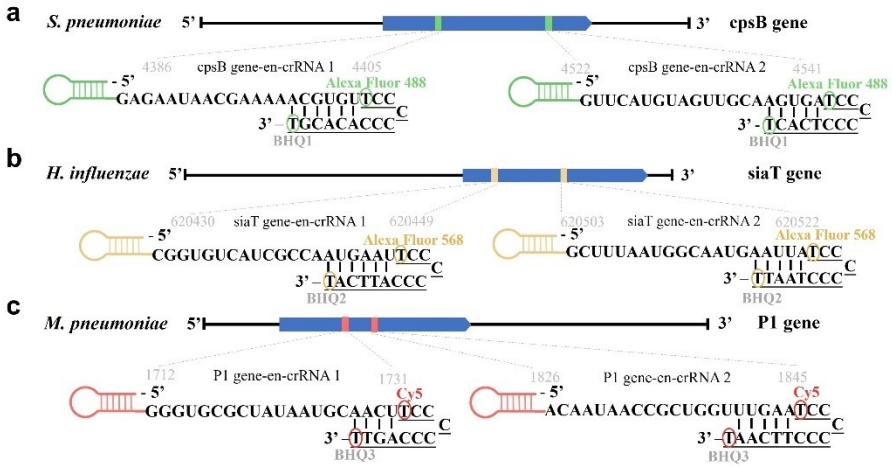

Figure S9. Schematic illustrations of the *cpsB* (a), *siaT* (b), and *P1* (c) gene maps depicting the selected loci for combined engineered crRNA.

2.10 The PAGE electrophoretic images of ERA products.

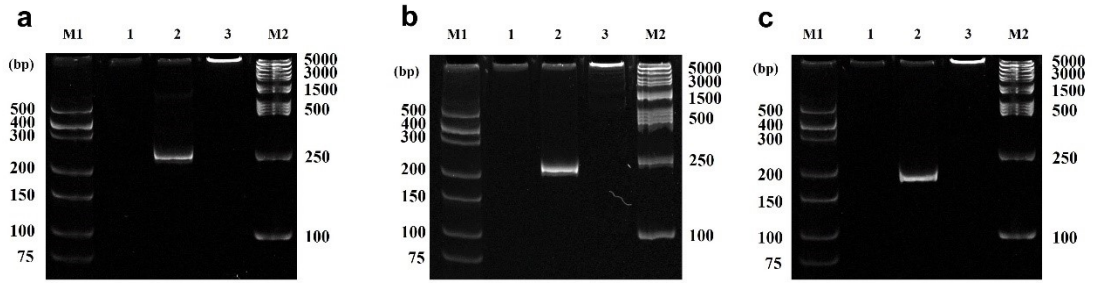

Figure S10. The PAGE electrophoretic images of ERA products. (a) The amplification of *cpsB* gene in *S. pneumoniae* is 248 bp. (b) The amplification of *siaT* gene in *H. influenzae* is 227 bp. (c) The amplification of *P1* gene in *M. pneumoniae* is 202 bp. Lanes 1, 2 and 3 correspond to no target control, the ERA product of target gene, and the corresponding gene plasmid, respectively. Lane M1 represents the DNA marker (25-500 bp). Lane M2 represents another DNA marker (100-5000 bp).

2.11 Schematic illustration of respiratory pathogen detections.

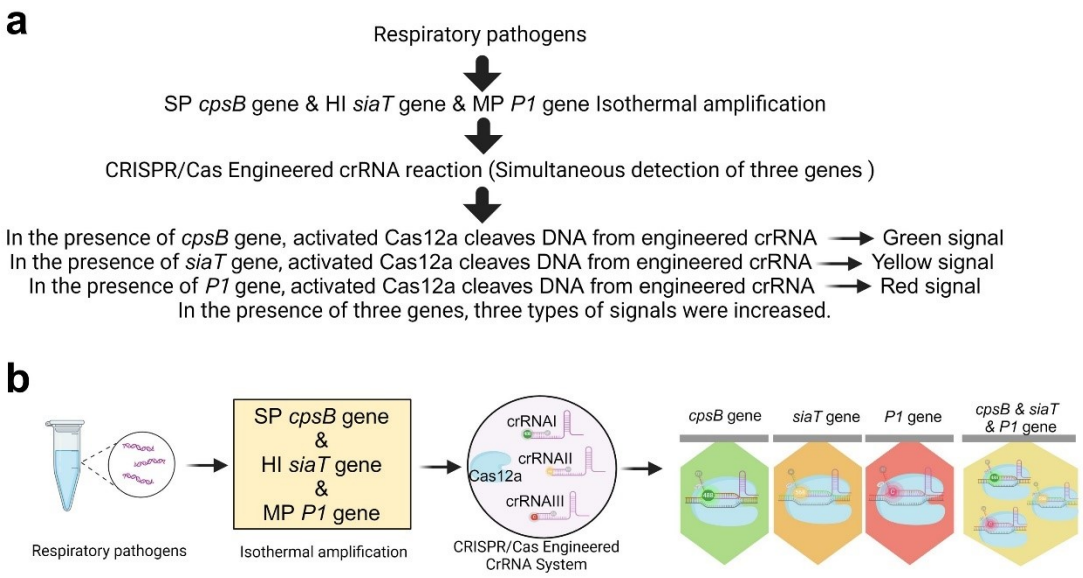

Figure S11. Schematic illustration of respiratory pathogen detections. (a) Experimental protocol and (b) detailed schematic illustration of *cpsB* gene, *sia T* gene, and *P1* gene identification using the CREM system. Illustrations created by Biorender.

2.12 The structure and image of the 3D printed device.

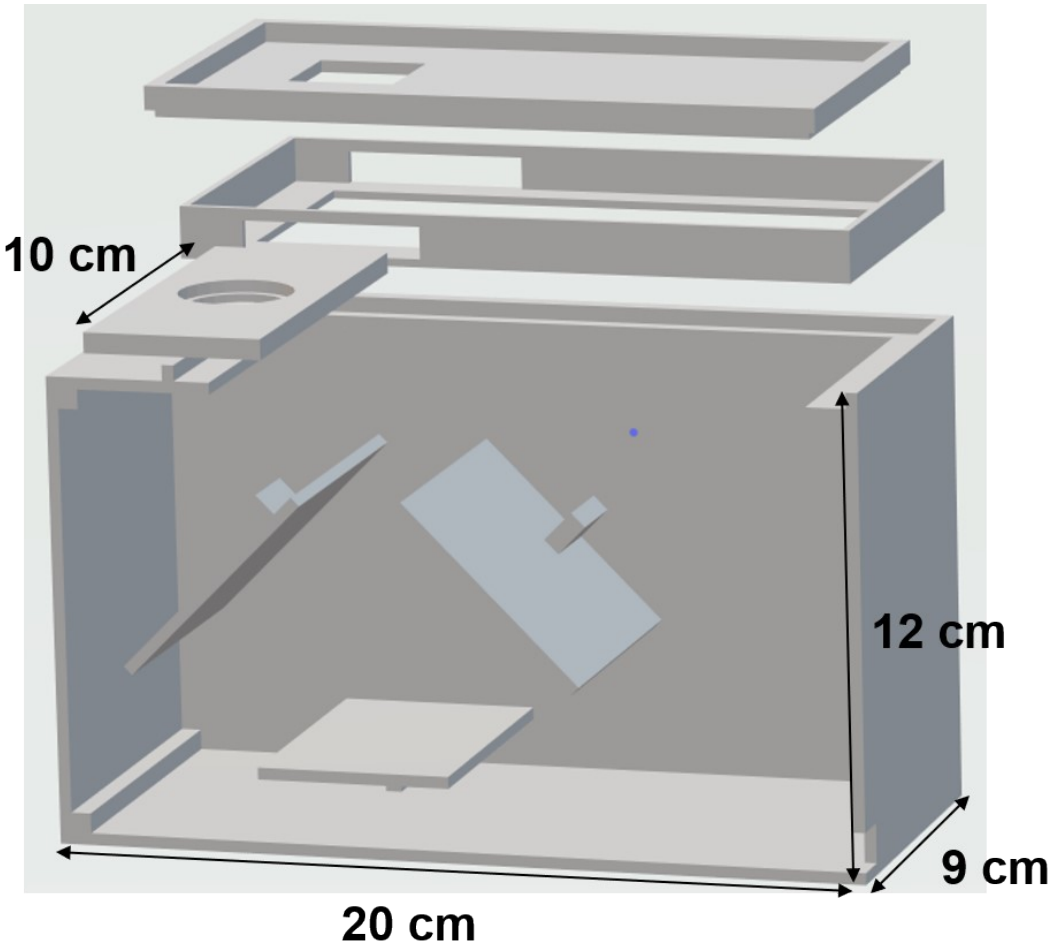

Figure S12. Detailed design of the 3D printed assembled equipment.

2.13 Results of three gene detections on chip.

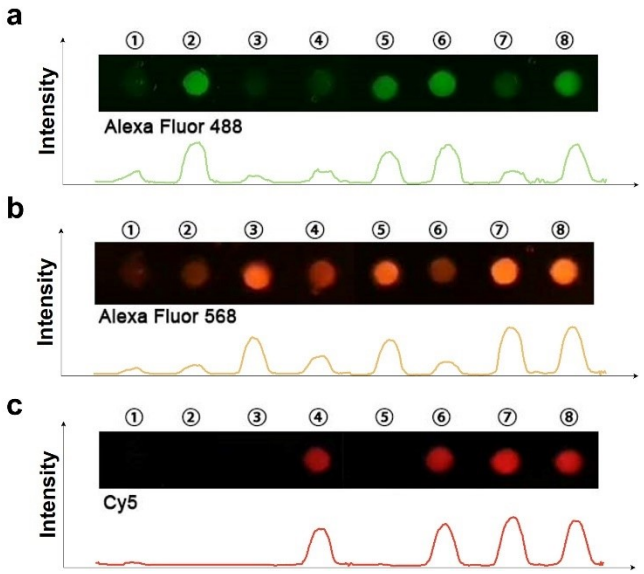

Figure S13. Results of three gene detections on chip. (a)Fluorescence images of *cpsB* gene were acquired with a 550/60 nm band pass emission filter. The Alexa Fluor 488 green fluorescent signal represents the *cpsB* gene of *S. pneumoniae* (2, 5, 6, and 8 wells). (b) Fluorescence images of *siaT* gene were obtained with a 605/55 nm band pass emission filter. The Alexa Fluor 568 orange fluorescent signal represents the *siaT* gene of *H. influenzae* (3, 5, 7, and 8 wells). (c) Fluorescence images of *P1* gene were captured with a 660/40 nm band pass emission filter. The Cy5 red fluorescent signal represents the *P1* gene of *M. pneumoniae* (4, 6, 7, and 8 wells).

2.14 Scatter plots of respiratory pathogen samples.

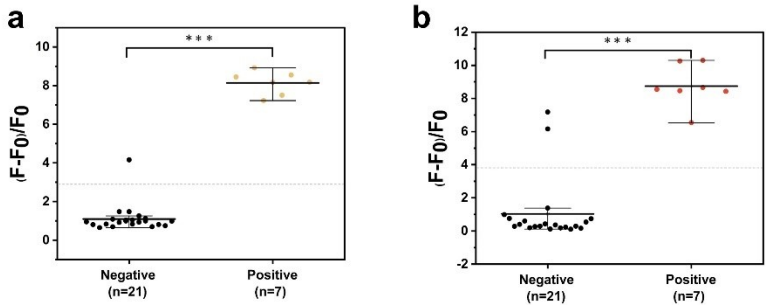

Figure S14. Scatter plots showing $(F-F_0)/F_0$ of 21 negative and 7 positive samples for *H. influenzae* in the Alexa Fluor 568 channel (a) and for *M. pneumoniae* in the Cy5 channel (b). The statistical significance of the data in a and b was determined using two-tailed unpaired Student's t-test (*** $p < 0.001$).

2.15 On chip detection of clinical samples.

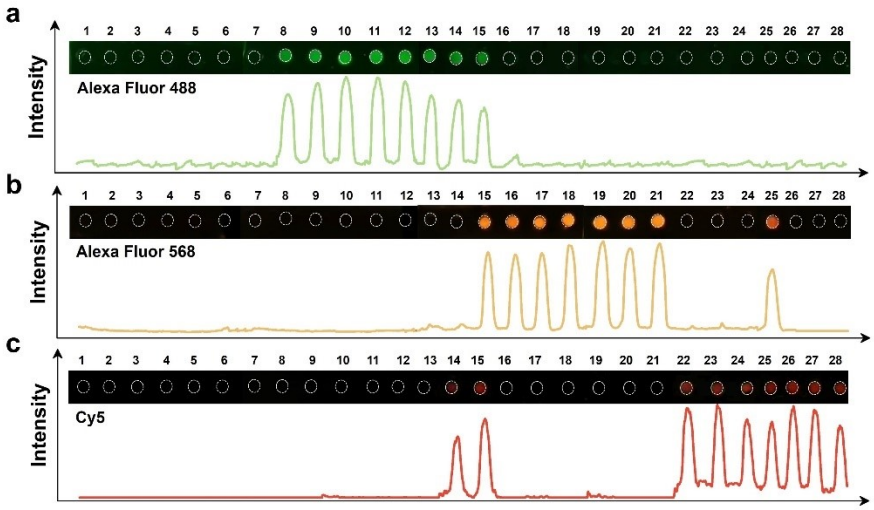

Figure S15. Results of clinical samples on chip. (a) Fluorescence images of *S. pneumoniae* were captured with a 550/60 nm band pass emission filter. (b) Fluorescence images of *H. influenzae* were acquired with a 605/55 nm band pass emission filter. (c) Fluorescence images of *M. pneumoniae* were acquired with a 660/40 nm band pass emission filter.

2.16 Fluorescence images of the clinical samples using the CREM system.

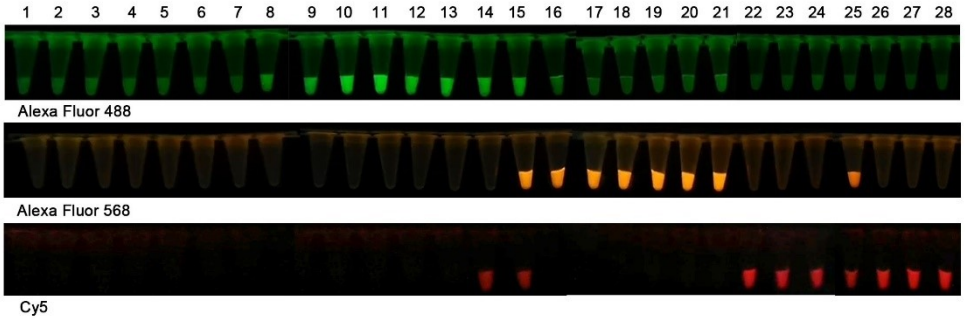

Figure S16. Fluorescence images of reaction tubes after the diagnosis of clinical samples using the CREM system. The specimens numbered 1-7 represent negative samples, while specimens numbered 8-14 indicate positive results for *S. pneumoniae*. Additionally, specimens numbered 15-21 show positive results for *H. influenzae* and specimens numbered 22-28 demonstrate positivity for *M. pneumoniae*.

2.17 qPCR of *S. pneumonia* detection.

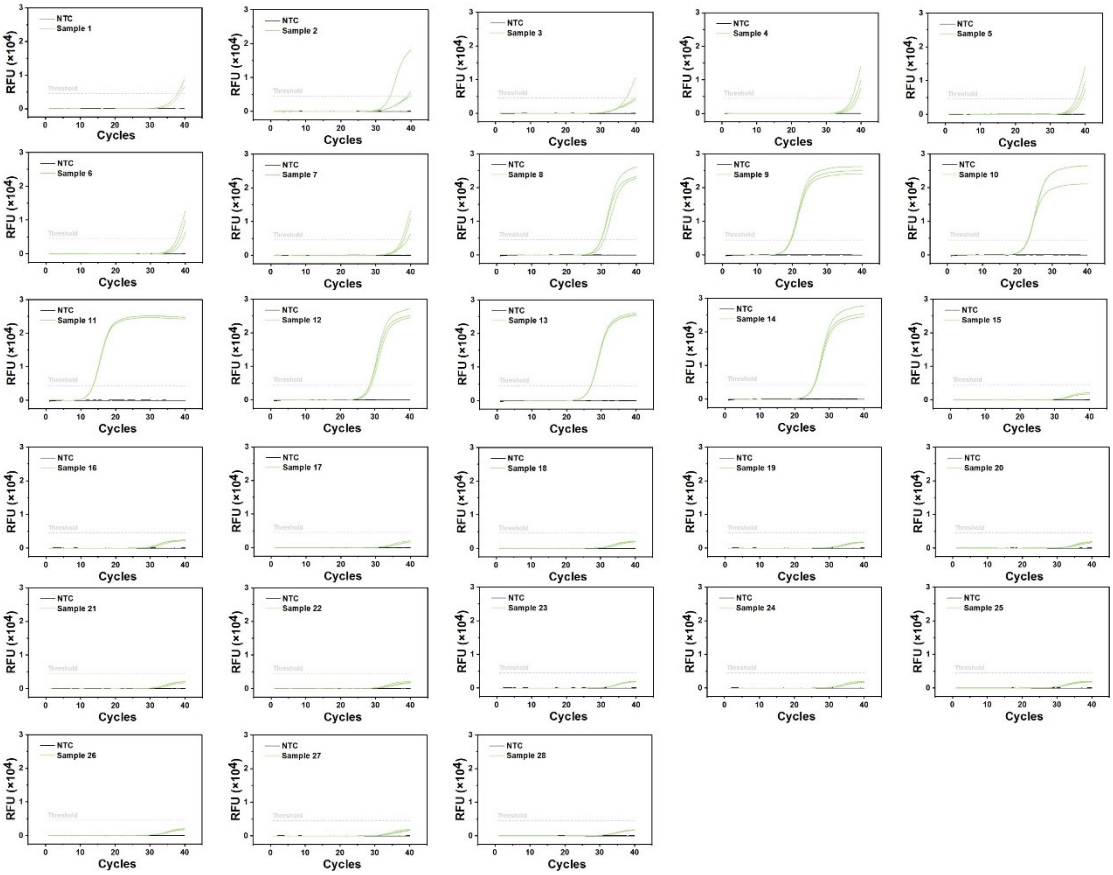

Figure S17. Clinical analysis of *S. pneumonia* by qPCR detection.

2.18 qPCR of *H. influenza* detection.

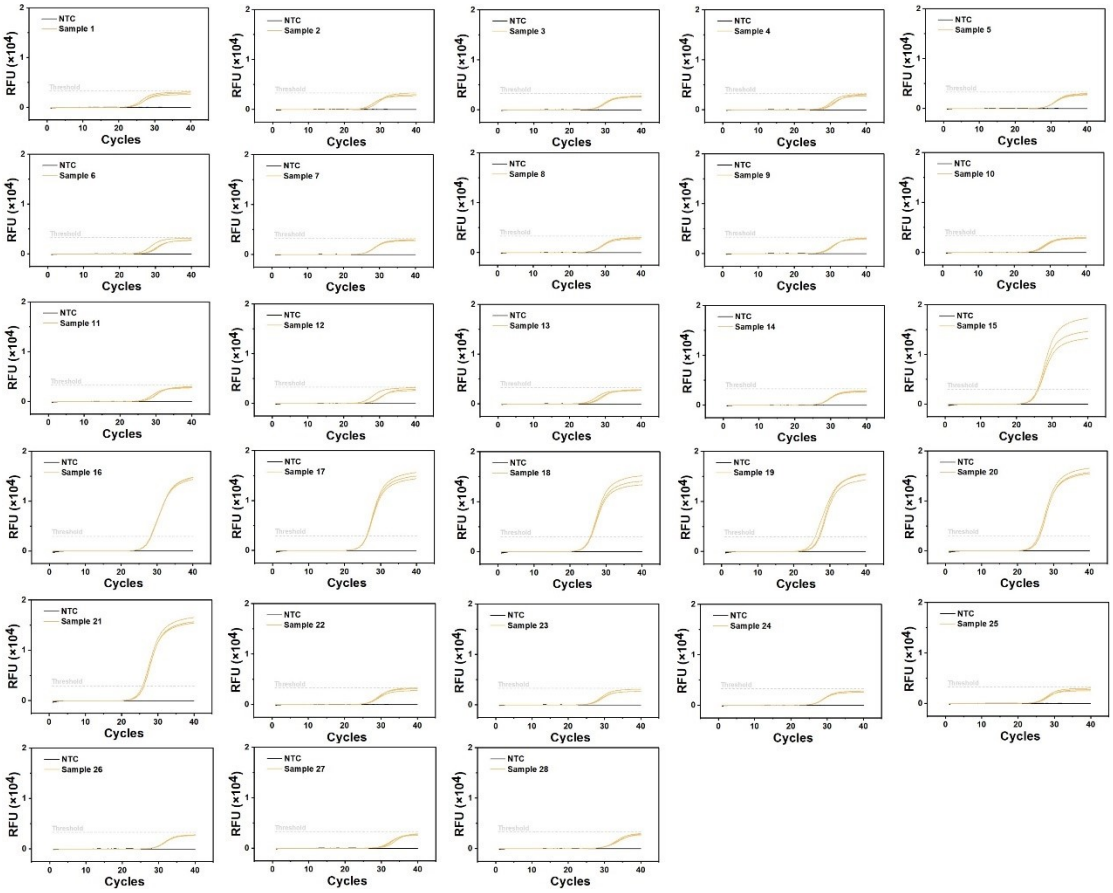

Figure S18. Clinical analysis of *H. influenza* by qPCR detection.

2.19 qPCR of *M. pneumoniae* detection.

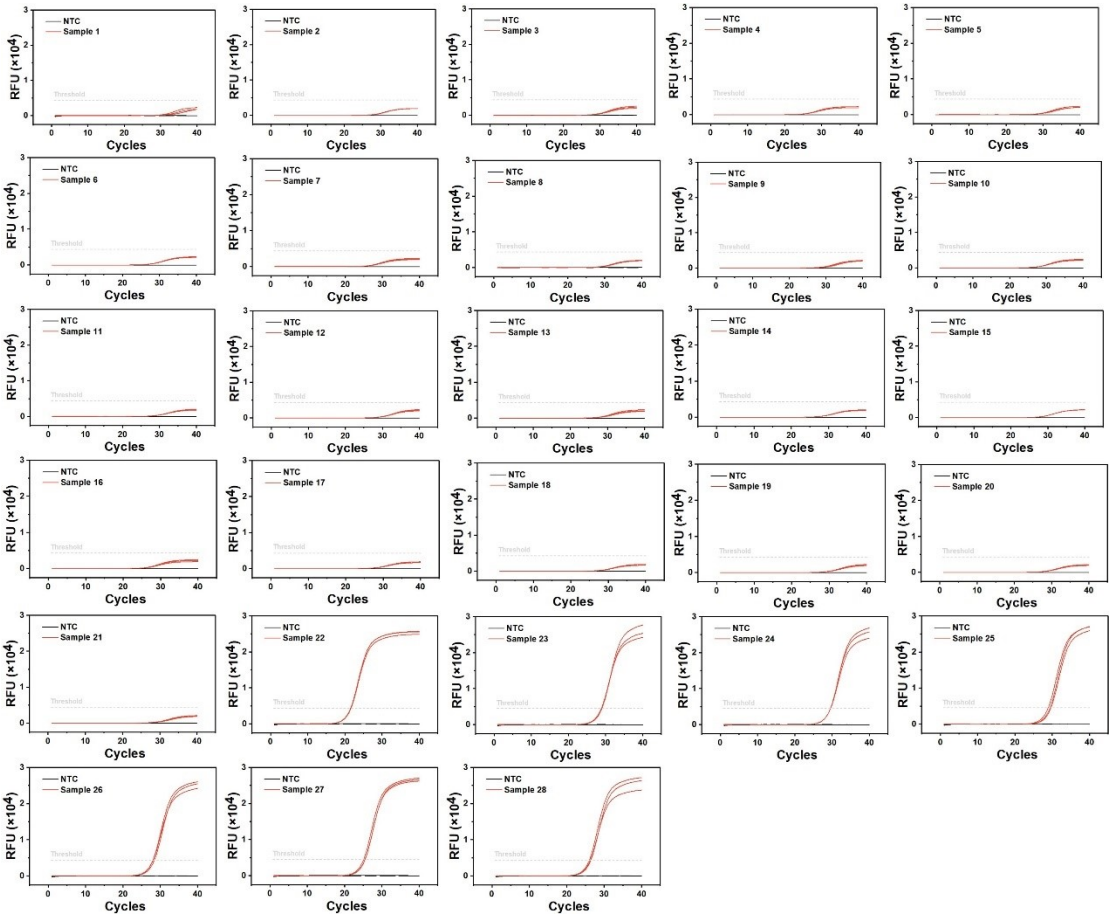

Figure S19. Clinical analysis of *M. pneumoniae* by qPCR detection.

3 Supplementary Tables

3.1 DNA sequences used in this study.

Table S1. DNA sequences used in this study.

Name	Sequence (5'-3')
A-primer-F	GCATTCCCAGTAGCACCCTT
A-primer-R	TCCCAATCTTCCTAACCACTGT
B-primer-F	ACAGAATACTTATTAAGTGCTGGCA
B-primer-R	ACACTAAGCAACTAGTAGCGAA
cpsB-primer-F	TGATGTTGGGAATCACGCCA
cpsB-primer-R	TGGAGGTCTACTGTCTAAATTGTG
siaT-primer-F	TGCGTGATGCTGGTTATGACG
siaT-primer-R	CTTGTGGCTTTTGGTGTACGTG
P1-primer-F	ACCAAGTCGGCCCACACC
P1-primer-R	CAGCAACTGCCATCCGTG
A-en-crRNA1	UAAUUUCUACUAAGUGUAGAUGCGCGCAGCAGGAG ACAGCA(Alexa Fluor 488)TCCCCCCTGCT(BHQ1)
A-en-crRNA2	UAAUUUCUAC<u>UAAGU</u>GUAGAU<u>CGCAUAUACAGCGA AGAAGA</u>(Alexa Fluor 488)TCCCCCCTCTT(BHQ1)
B-en-crRNA1	UAAUUUCUACUAAGUGUAGAUAAUAUUACUUAUAG GGAUGG(Cy5)TCCCCCCAT(BHQ3)
B-en-crRNA2	UAAUUUCUACUAAGUGUAGAUGAAAGAACAAUACG CAAAGA(Cy5)TCCCCCCTCTT (BHQ3)
en-crRNAII	UAAUUUCUACUAAGUGUAGAUAAUAUUACUUAUAG GGAUGG(Cy5)T(Cy5)TCCCCCCCAT(BHQ3)
cpsB-en-crRNA1	UAAUUUCUACUAAGUGUAGAUGAGAAUAACGAAAA ACGUGU(Alexa Flour 488)TCCCCCCACACGT(BHQ1)
cpsB-en-crRNA2	UAAUUUCUAC<u>UAAGU</u>GUAGAU<u>GUUCAUGUAGUUGC AAGUGA</u>(Alexa Flour 488)TCCCCCCTCACT(BHQ1)
siaT-en-crRNA1	UAAUUUCUAC<u>UAAGU</u>GUAGAUCGGUGUCAUCGCCA AUGAAU(Alexa Fluor 568)TCCCCCCATTCAT(BHQ2)
siaT-en-crRNA2	UAAUUUCUAC<u>UAAGU</u>GUAGAU<u>GCUUUAAUGGCAAU GAAUUA</u>(Alexa Fluor 568)TCCCCCCTAATT(BHQ2)
P1-en-crRNA1	UAAUUUCUACUAAGUGUAGAUGGGUGCGCUAUAAU GCAACU(Cy5)TCCCCCCAGTT(BHQ3)
P1-en-crRNA2	UAAUUUCUACUAAGUGUAGAUACAAUAACCGCUGG UUUGAA(Cy5)TCCCCCCTTCAAT(BHQ3)
Target A plasmid	ATGGCTTTTTCTATCGGTGAATTTTCCGAACTAGTAG GCATTCCCAGTAGCACCCTTAGATTCTACGAAAAAGA AGGCTTAATAACCCCTGACCGCGACAAGAATAA**<u>TTT G</u>CGCATATACAGCGAAGAAGA**CGCCAATTGGCTAA AATTTTTACTGCACTTAAAAGGCGCCGGGTTATCGGT AGAAGAATTAAAGCAGTACACAA**<u>TTTG</u>GCGCGCAG CAGGAGACAGCA**CTATTTCCGAACGATTAAATATGT

	TAAAAAAGAAAAAGGTTATTTTGGAGCAAGAGATTG AAGACTTGCAGAAGAATTTGGATACAGTGGTTAGGA AGATTGGGATTTATGAAGAGAAGGTTAAGACTAGAC GAGTTTAG
Target B plasmid	CAGAATACTTATTAAGTGCTGGCATATGTATGGCAAT TG**TTTCAATATTACTTATAGGGATGG**CTATCAGTAA TG**TTTCGAAAGAACAATACGCAAAGA**GGTTTTTCTT TTTCGCTACTAGTTGCTTAGTGTTAACTTTAGTTGTAG CTTCAAGTCTAAGTAGCTCAGCAAATGCATCACAAAC AGATAATGGCGTAAATAGAAGTGGTTCTGAAGATCC AACAGT
CpsB plasmid	AGCAATATTTTGATGTTGGGAATCACGCCAGTAATTG CTCATATTGAACGTTATGATGC**TTTGGAGAATAACG AAAAACGTGT**TCGTGAACTGATTGATATGGGGTGCT ATACTCAGATAAATAGTTATCATGTTTCAAAACCTAA GTTCTTTGGTGAAAAATATAAATTCATGAAAAAGAGA GCTCGGTATTTTTTGGAACGTGA**TTTAGTTCATGTAG TTGCAAGTGA**CATGCACAATTTAGACAGTAGACCT
siaT plasmid	CAGGAGGAATGGGACACGTTAATATCGGCGCAAGTT TATTATTTTCAGGTATGTCAGGATCCGCATTAGCTGA TGCAGGCGG**TTTAGGTCAGCTTGAGATTAAAGC**AA TGCGTGATGCTGGTTATGACGATGATATTTGCGGAGG AATTACTGCTGCTTCTTGTATTATTGGGCCATTAGTTC CACCAAGTATTGCAATGATTATTTACGGTGTCATCGC CAATGAATCTATCGCAAAACTCTTTATTGCAGGTTTT ATTCCCGGTGTATTAATTAC**TTTAGCTTTAATGGCAA TGAATTA**TCGCATTGCAAAAAAACGAGGTTATCCAC GTACACCAAAAGCCACAAGAGAACAACTTTGCAGCA GCTTTAAACAATCTTTTTGGGCAA
P1 plasmid	ACCTGGTTCGGGCAAGCGCTTTTGGTGTTTGGTGGCA ATGGCCATGTTACCAAGTCGGCCCACACCGCGCCTTT GAGTATAGGTGTC**TTTAGGGTGCGCTATAATGCAA CT**GGTACCAGTGCTACTGTAACTGGTTGACCATATGC CTTACTGTTCTCAGGCATGGTCAACAAACAAACTGAC GGGTTAAAGAATCTACCC**TTTAACAATAACCGCTGG TTTGAA**TATGTACCACGGATGGCAGTTGCTGGCGCTA AGTTCGTTGGTAGGGAACTCGTTTTAGCGGGTACCAT TACCATGGGTGATACCGCTACCGTACCTCGCTTACTG TACGATGAACTTGAAAGCAACCTGAACTTA

3.2 Comparison of other CRISPR-Cas assays.

Table S2. Comparison of different nucleic acid diagnostic techniques in pathogen

detection (unit: copies/μL).

Methods	Target	Pre-amplification	Turnaround time (min)	Limit of detection	Portable Detection	Ref.
mCARMEN	Respiratory viruses	RT-PCR	> 120	10	No	2
-	*Salmonella*	PCR	120	10	-	3
LAMP-LFA	*M. pneumoniae*	LAMP	90	600	Yes	4
ERA/ Cas12a	*M. pneumoniae*	ERA	50	200	Yes	5
Cas-gold	ASFV*	RPA	> 90	200	Yes	6
TL-LFA	SARS-CoV-2*	RT-RPA	60	100	Yes	7
LIAMT	SARS-CoV-2; HIV*	RT-RPA	90	100	Yes	8
Plasmonic RPA chip	Coronavirus *hMPV**	RT-RPA	40	1000	No	9
CREM	*S. pneumonia; H. influenza; M. pneumoniae*	ERA	80	100	Yes	This study

*ASFV: African swine fever virus; SARS-CoV-2: Severe acute respiratory syndrome coronavirus 2; HIV: Human immunodeficiency virus; *hMPV:* Human metapneumovirus.

4 Supplementary References

(1) Xia, S. and X. Chen, *Cell Discovery.* **2020**, 6, 37.

(2) Welch, N.L., M. Zhu, C. Hua, J. Weller, M.E. Mirhashemi, T.G. Nguyen, S. Mantena, M.R. Bauer, B.M. Shaw, C.M. Ackerman, S.G. Thakku, M.W. Tse, J. Kehe, M.-M. Uwera, J.S. Eversley, D.A. Bielwaski, G. McGrath, J. Braidt, J. Johnson, F. Cerrato, G.K. Moreno, L.A. Krasilnikova, B.A. Petros, G.L. Gionet, E. King, R.C. Huard, S.K. Jalbert, M.L. Cleary, N.A. Fitzgerald, S.B. Gabriel, G.R. Gallagher, S.C. Smole, L.C. Madoff, C.M. Brown, M.W. Keller, M.M. Wilson, M.K. Kirby, J.R. Barnes, D.J. Park, K.J. Siddle, C.T. Happi, D.T. Hung, M. Springer, B.L. MacInnis, J.E. Lemieux, E. Rosenberg, J.A. Branda, P.C. Blainey, P.C. Sabeti, and C. Myhrvold, *Nature Medicine* **2022**, 28, 1083-1094.

(3) Shanmugasamy, M., T. Velayutham, and J. Rajeswar, *Vet. World.* **2011**, 4, 562-564.

(4) Wang, Y., Y. Wang, W. Jiao, J. Li, S. Quan, L. Sun, Y. Wang, X. Qi, X. Wang, and A. Shen, *AMB Express.* **2019**, 9, 196.

(5) Deng, Z., H. Hu, D. Tang, J. Liang, X. Su, T. Jiang, X. Hu, W. Ying, D. Zhen, X. Xiao, and J. He, *Front. Microbiol.* **2022**, 13, 811768.

(6) Lu, S., F. Li, Q. Chen, J. Wu, J. Duan, X. Lei, Y. Zhang, D. Zhao, Z. Bu, and H. Yin, *Cell Discovery.* **2020**, 6, 18.

(7) Xiong, E., L. Jiang, T. Tian, M. Hu, H. Yue, M. Huang, W. Lin, Y. Jiang, D. Zhu, and X. Zhou, *Angew. Chem., Int. Ed.* **2021**, 60, 5307-5315.

(8) Li, Z., S. Zhang, J. Zhang, L. Avery, D. Banach, H. Zhao, and C. Liu, *Adv. Sci.* **2024**, n/a, 2310066.

(9) Woo, A., H.S. Jung, D.-H. Kim, S.-G. Park, and M.-Y. Lee, *Biosens. Bioelectron.* **2021**, 182, 113167.